

Contribution of the covalent component of the hydrogen-bond network to the properties of liquid water

Yifei Shi, Hayden Scheiber, and Rustam Z. Khaliullin

Department of Chemistry, McGill University, 801 Sherbrooke St. West, Montreal, QC H3A 0B8, Canada

Many remarkable properties of liquid water originate from the ability of water molecules to form hydrogen bond, which is a combination of electrostatic, induction, dispersion and covalent interactions. In this work, we developed an *ab initio* molecular dynamics method that enabled us to adjust the spatial extent of the covalent component of interactions between water molecules in simulations. We show that for room-temperature liquid water, a seemingly small amount of electron transfer has a profound effect on observable properties of liquid water. In particular, the tetrahedral structure, O-H stretch mode and viscosity are all significantly determined by covalent interactions.

PACS numbers:

INTRODUCTION

Detailed understanding of the physical nature of hydrogen bonding (HB) between molecules in water is essential for unraveling origins of unique physical and chemical properties of this ubiquitous and important liquid. Since the dawn of quantum mechanics, it has been known that hydrogen bonding is a complex phenomenon that arises from the interplay of several distinct effects: interaction between molecules permanent multipoles (dipoles, quadrupoles, etc.), polarization, dispersion, and orbital donor-acceptor interactions [1].

Donor-acceptor interaction leads to the transfer of the electron density between molecules and, therefore, is called the charge-transfer or covalent component of HB. The concept of covalent interactions in HB has always been tremendously useful in chemistry as it helps explain, to name only few, water’s unique properties as a solvent, its ability to catalyze a wide variety of chemical processes, and strong cooperativity between hydrogen bonds. From the theoretical standpoint, the covalent component of HB has attracted significant attention because of its purely quantum mechanical nature, which, unlike electrostatic and dispersion interactions, is hard to describe with simple analytical potentials [?].

Recent developments in energy decomposition techniques based on accurate electronic structure methods have helped make substantial progress towards quantifying the individual contributions of various physical effects to the HB energy in small water clusters. However, the extent of intermolecular charge transfer in HB has remained the last unresolved issue until recently [2–4]. Natural bond orbital analysis[5] and natural energy decomposition analysis [6] have suggested that charge transfer is the major component of HB [7–9] because, if charge transfer is neglected, these methods show no binding at the water-dimer equilibrium geometry. After a debate spanning several decades, it has been argued that natural bond orbital analysis is not optimal for weak interactions [4]. It appears that the covalent component of HB

is better described by early decomposition methods [10?–14] as well as their modern variants [15–17]. According to these methods, charge transfer contributes only around 20% to the overall binding energy between water molecules in small clusters [13, 14, 18–20], in agreement with the with chemists’ long-held intuitive view of HB.

While energy decomposition methods have helped understand the importance of the charge-transfer for the binding strength in gas-phase water clusters little is known about the contribution of the covalent component of HB to the *observed* properties of liquid water. A great fundamental importance of studying covalency of HB has been pointed in several works that noted a deep connection between the covalent interactions and features of the X-ray absorption [21], infrared [22], and nuclear magnetic resonance [23] spectra of liquid water. In this work, we extended a recently developed energy decomposition method for periodic systems [24] to perform an unprecedented *ab initio* molecular dynamics study that measures quantitatively the contribution of the covalent component of HB to the structural, dynamical and spectroscopic properties of liquid water at ambient conditions. Our results show that a seemingly insignificant covalent component of HB is defining of the properties of liquid water.

METHODS

To quantify the influence of the covalent component of HB on the observed properties of liquid water we compared the properties calculated using *ab initio* molecular dynamics (AIMD) based on two different models. The first model model incorporates the intermolecular covalency fully whereas the second removes it completely.

The first model is the conventional Kohn-Sham density functional theory (DFT), in which electrons of a water molecule delocalize over all neighbors. This model is known to reproduce properties of liquid water reliably, in semi-quantitative agreement with experimental measurements. In this work, this model is referred to as

delocalized-electron, reference, or realistic model.

The second model is a constrained DFT method based on absolutely localized molecular orbitals (ALMO) [25]. Unlike conventional DFT, ALMO DFT [24] is able to confine each electron strictly to its own molecule and therefore completely remove the covalent component from intermolecular bonding. Mathematically, this is achieved by expanding Kohn-Sham molecular orbitals *only* in terms of the atomic orbitals of the same molecules [25? ?]. Such molecular orbitals are called absolutely localized because they are localized on molecules in the same sense as atomic orbitals are localized on atoms. To shorten the discussion, intermolecular interaction without the covalent component are referred to as *devalent* interactions and the ALMO-based model is called localized-electron or *devalent* model. It is important to note that this model retains all other physical effects, including the covalent component of *intramolecular* OH bonds. To ensure that the covalent component of intermolecular bonding is removed accurately we performed several tests described in the Supplementary Information.

To keep electrons absolutely localized in a course of AIMD simulations, we extended the recently developed ALMO DFT method for condensed molecular systems [24] so that the analytical forces can be computed directly from the ALMO DFT energies (see Supplementary Information).

All AIMD simulations, with delocalized and localized molecular orbitals, were performed using the dispersion-corrected [26] BLYP exchange-correlation functional [27] and TZV2P basis set [28]. The temperature of simulations was set to 298 K. The size of a periodic cubic simulation box was fixed to reproduce the experimental $0.997 \text{ g}\cdot\text{cm}^{-3}$ density of ambient liquid water. Since removing intermolecular covalency can affect the density, we also performed a set of simulations for a system, which density was adjusted to 1 atm using constant pressure AIMD. The length of the AIMD simulations was chosen to obtain statistically meaningful results. A detailed description of the calculations is presented in the Supplementary Information.

Temperature and potential are “two peas in a pod”. Removing covalent interactions weakens HBs. Can we recover properties of room-temperature liquid water using the devalent model at lower temperature? The same question can be asked another way: is devalent room-temperature water completely equivalent to high-temperature covalent water? We know the exact contribution of covalency to the binding energy of molecules. How much the temperature should be adjusted to keep the average Boltzmann weights the same?

RESULTS AND DISCUSSION

All figures must be in vector format. You could use, for example, the following lines in the gnuplot scripts
 set terminal postscript eps color enhanced size Xsize, Ysize
 set output 'filename.eps'

Do the calculations and plug in the numbers below.

Variational principle of quantum mechanics guarantees that removing covalent interactions weakens intermolecular bonding. ALMO-based decomposition energy analysis predicts that, in a water dimer, the transfer of 0.27% of an electron contributes $\sim 7.0 \text{ kJ}\cdot\text{mol}^{-1}$ (37%) to the overall stabilization of the hydrogen bond at equilibrium geometry, in agreement with earlier reports [13, 14, 18]. This contribution is higher in the *cooperative* HB network of liquid water at ambient conditions **calculated in this work**: 1.1% of electron and $19 \text{ kJ}\cdot\text{mol}^{-1}$ per hydrogen bond, **which agrees with previous study** [29].

Molecular structure. The covalent component of weak intermolecular bonds has only a minor effect on much stronger intramolecular bonds. The average length of intramolecular OH bond changes from 2.33 Å in the realistic model to 2.75 Å in the devalent model of water. At the same time, the average intramolecular HOH angle changes from 105.5 degrees to 104.3 degrees[, becoming closer to the value calculated for the 298 K gas phase water molecule].

The effect of the covalency on the structure of the HB network is far more pronounced. The oxygen-oxygen radial distribution function (RDF) in Figure 1A shows that weaker intermolecular interactions without the covalent component lead to the considerable expansion of the first coordination shell of a water molecule from the “realistic” average of 2.8 Å to 3.1 Å. The shift of the first-shell peak is accompanied by its broadening that is indicative of a wider variety configurations available to devalent HBs.

These dramatic changes in the structure of the HB network are consistent with the decrease in the HB strength. It is remarkable, however, that the remaining components of HB – permanent electrostatic, polarization and dispersion – are sufficiently strong to retain several characteristic structural features of the network: well-defined coordination shells and directional HBs [30]. Indeed the second coordination peak in the RDF of the devalent model remains clearly visible though shifted to higher distances. The distribution of HB angles still has a maximum at 0° despite becoming broader (Figure 1B).

The structure of the HB network for both models can also be illustrated with the spacial distribution of oxygen atoms around a reference water molecule (Figure 2). It shows that the distorted tetrahedral structure of liquid water is retained without the covalent component (cf. Figure 2A and B), indicating that permanent electrostatic and polarization interactions tend to orient water molecules the same way as the charge-transfer interaction. For comparison, if a model neglects electrostatic interactions includes only the

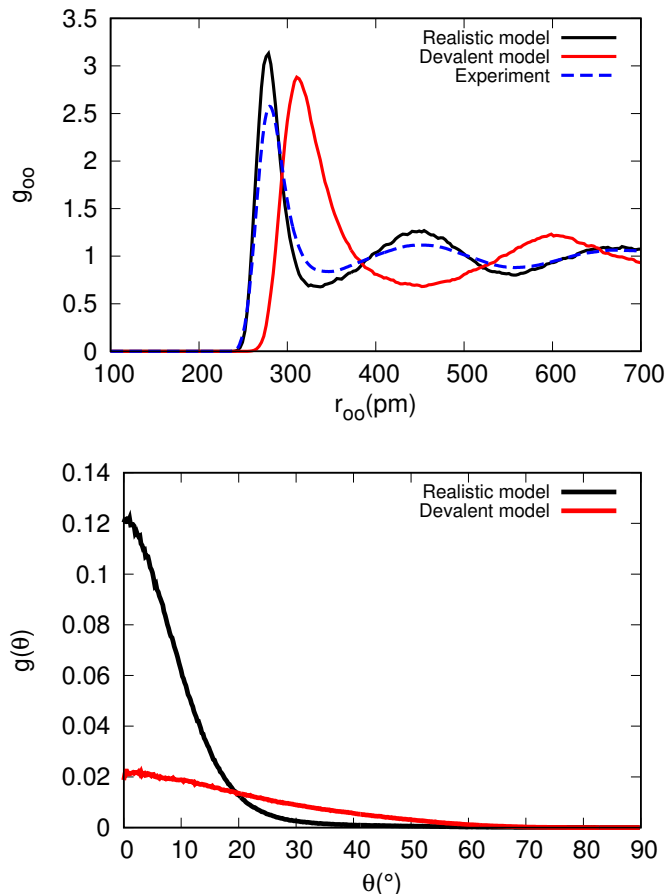


FIG. 1: A. Oxygen-oxygen radial distribution function. Color coding throughout the manuscript: realistic - black, devalent - red, experiment - black dash, vapor - blue, devalent NPT - blue (these colors make it easier for color blind persons to read figures and at the same time minimize the publication cost). Legends throughout: “Realistic model”, “Devalent model”, “Experiment”. Decrease panel height. See figure guidelines for Nature Chemistry. B. Angular distribution of the H-O...O angle. The distribution is computed for hydrogens within 2.3 Å from a reference molecule. Compute as we discussed. Can we compare the angular distribution to the experimental curve?

Lennard-Jones potential, which represents dispersion interactions and short-distance repulsion, the HB becomes truly non-directional with uniform angular distribution (Figure 2C).

==== STOPPED HERE =====

The importance of permanent electrostatics for the structure of liquid water has been used since the birth of molecular mechanics to create and fine-tune electrostatic fixed-charge models of water. Although such models reproduce the structure and many important properties of liquid water they neglect the covalent component of ZZZ.

At this point, it is appropriate to comment on the ability of the reference model to reproduce properties of water. [GGA is known to underestimates the energy

gap slightly. As a result they overestimate the electron delocalization, overbinds molecules, produces RDF with sharper peaks than those derived in X-ray scattering experiments. Underestimated diffusion constant, overestimated viscosity. However, for all calculated properties the imperfections of the reference model are far less significant than the changes induced by neglecting intermolecular covalency. This is the main reason we are confident that our devalent model is an accurate depiction of the contribution of the covalent component to the properties.]

The O-O peak seems to depend only on the interaction strength. Here the density is the same for both systems, but the molecules seem to get further away. While for the results shown in Fig 8 the densities are different but the peaks are at the same position. How to interpret this?

ALMO water Density is decreased by ZZZ % to ZZZ g/cm³. While this is a noticeable drop It is important to emphasize that the retained components like permanent multipoles and polarization effects are sufficiently strong to keep the NOCOV water liquid.

We also show in Fig 3, how many HBs a molecule donate(D) or accept(A), with a geometric criterion that the H-O-O angle is smaller than 30° and the O-O distance is smaller than 3.5Å. The number of HBs is 35% less in the localized system.

Network statistics and dynamics. The HB decay function $C_{HB}(\tau)$ is defined as:

$$C_{HB}(\tau) = \frac{\sum_{i,j} \langle \theta_{ij}(\tau) \theta_{ij}(0) \rangle}{\sum_{i,j} \langle \theta_{ij}(0) \theta_{ij}(0) \rangle} \quad (1)$$

where $\theta_{ij}(\tau)$ equals to 1 if there is a HB formed between molecule i and j through out the time period of $t = 0$ to $t = \tau$. At large enough time it should decay exponentially, and the HB life time τ_{HB} is defined as the rate of decay: $C_{HB}(\tau) \sim e^{-\tau/\tau_{HB}}$. The HB decay function is shown in Fig 4.

The calculated HB life time for delocalized system is 0.7ps, and for localized system it becomes 0.08ps, indicating that HB are much less stable without covalent interaction.

Diffusion constant and viscosity. D and η were calculated using the method of ZZZ [32]. The result is listed in Tab I. For delocalized reference the calculated viscosity is larger than the experimental value, a consequence of overestimating interaction strength in the XC functional. And it also implies that about 90% of water’s viscosity comes from covalency.

Molecular dipole moment and dielectric constant. Water is a unique solvent. In spite of the ambiguity of the definition of a local dipole moment, we assign each electron to one molecule through the method of maximally localized Wannier centers (MLWC). The resulting dipole distribution is shown in Fig 6. The average dipole moment of a water molecule is 3.09 Debye for

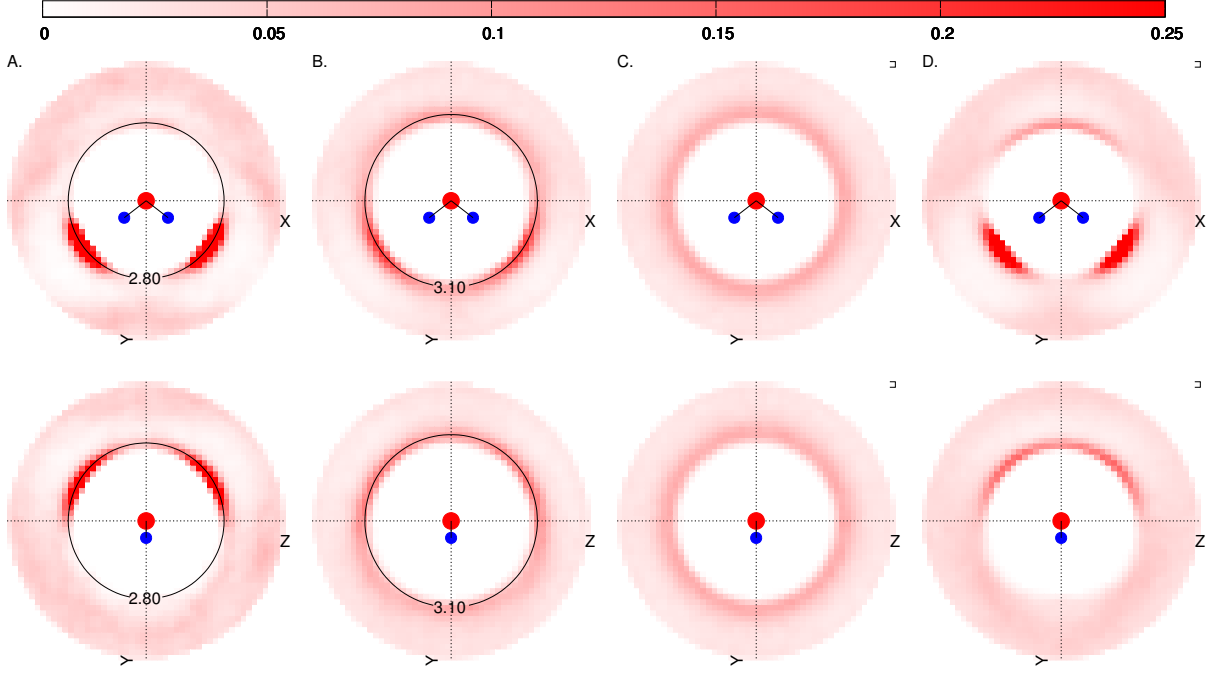


FIG. 2: Cross sections of the spacial distribution of oxygen atoms. The upper panels show the cross section of the spacial distribution function in the plane of the reference water molecule, whereas the lower panels show the cross section in the plane dissecting the molecule. A. Reference model, B. localized model, C. Modified TIP3P model that include only van der Waals interactions, D. TIP3P model [31]: electrostatic interaction between atomic point charges combined this van der Waals interactions [31].

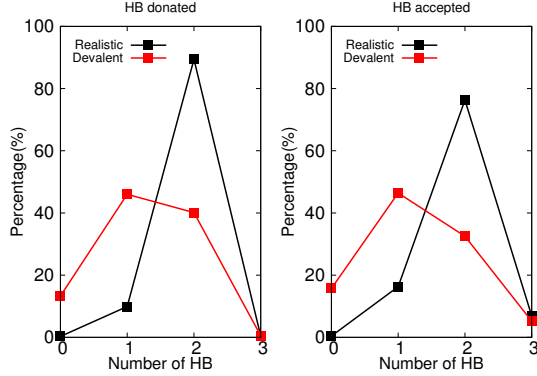


FIG. 3: HB statistics for liquid water with and without inter-molecular covalency. **Replace with a graph. Two panels one for accpetor, one for donor. 2 lines with points on each panel: covalent and devalent.**

delocalized system and 2.47 Debye for localized system, while for an isolated molecule it is 1.96 Debye. **Covalent interaction is also partially responsible for the increase of dipole moment from gas to the condensed phase.** The dielectric constant can be calculated through the fluctuation of the total dipole moment[33, 34]:

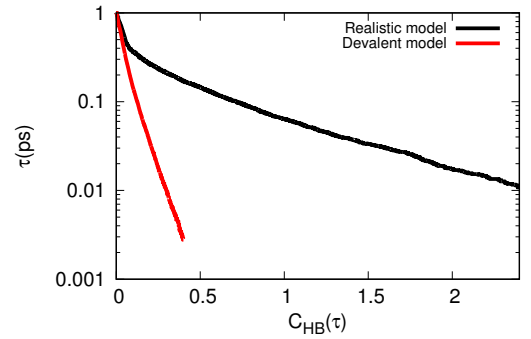


FIG. 4: HB decay function for delocalized reference and localized system.

TABLE I: Viscosity and diffusion constant

	$D(\text{\AA}^2/\text{ps})$	$\eta(\text{Pa} \cdot \text{s})$
Localized	0.7188	3.5×10^{-4}
Delocalized	0.1069	2.95×10^{-3}
Experimental	0.239	8.9×10^{-3}

$$\epsilon = 1 + \frac{4\pi}{3Vk_B T} (\langle |\vec{M}|^2 \rangle - \langle \vec{M} \rangle^2) \quad (2)$$

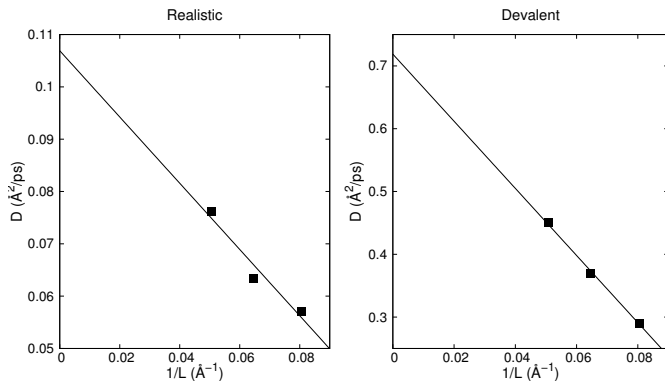


FIG. 5: Diffusion constant as a function of the system size, for 64, 125 and 256 water molecules. The square dots are from simulation and solid line is a linear fit. **error bars?**

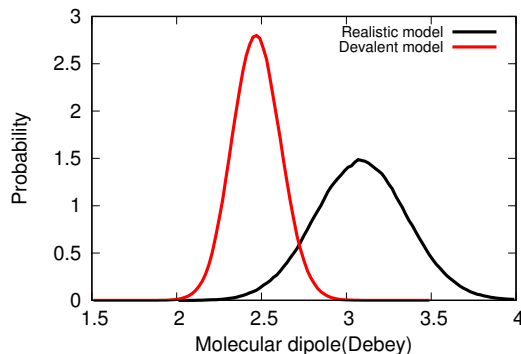


FIG. 6: Dipole distribution of water molecules

where V is the volume of the system and \vec{M} the total dipole. The dielectric constant for the realistic model is 70, close to the experimental value of 78. For the devalent model, this value increases to 180.

Infrared spectrum. Fig 7 shows the infrared (IR) spectrum of the localized and reference systems. For comparison, the IR spectrum of none-interaction water vapor is also shown. The O-H stretch modes (also denoted by ν band) of the localized system do not show the broadening and shift due to HBs, as in the delocalized system. And now the two peaks for symmetric and asymmetric stretch modes are separate. This implies that these modes are very sensitive to covanlency, and without covanlency, they are very similar to that of the none-interacting molecules. **However, the integrated intensity of the ν band is still ~ 10 times larger than that of water vapor, which is generally an indication of the existence of HBs.** Another difference between the localized and delocalized system is the intermolecular modes, they are shifted to lower energy because the intermolecular bonding in localized system is weaker. The bending modes remain roughly the same for localized, delocalized and vapor systems. Since in liquid water, the shift of the centre of ν band is caused by the coupling between the O-H stretch mode

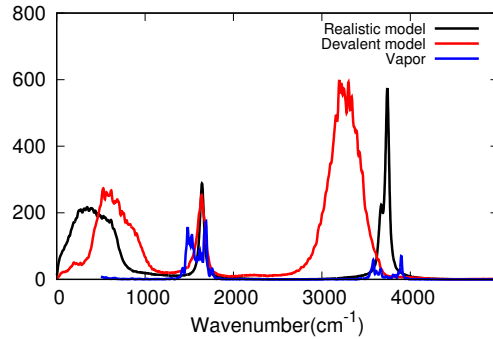


FIG. 7: IR spectrum. For water vapor, localized and delocalized systems. The low wavenumber part of the spectrum for vapor which corresponds to rotational modes are not shown for simplicity. The O-H stretch mode ($\sim 3600 \text{ cm}^{-1}$) for localized system is very similar to vapor which is none-interaction. And the intermolecular modes ($\sim 500 \text{ cm}^{-1}$) moves to the left, indicating the intermolecular bonding is weaker.

and librations [35], it then implies that this coupling is mainly through covalent interactions. Furthermore, the ν band is very narrow, while the relative position and orientation of neighboring water molecules are larger (as shown in Fig 1B), this also implies that the HBs are now much less sensitive to molecular environment.

Conclusions. In this work, we present the effect of the covalent interaction on observable properties of liquid water, and show that although the charge transfer energy only makes up 30% of the total bonding energy, it plays a dominant rule in some other properties, like the OH stretch mode, viscosity, HB life time. And also significantly changes dipole moment, angular distribution.

Our result also suggest that classical models that don't take account of covalency only have limit applicability, as they fine-tune the parameters only for certain conditions.

Implications: shows that ALMO-based AIMD is an excellent tool for the nature of intermolecular bonding in other condensed phase systems. Catalysis, solvation.

SUPPLEMENTARY INFORMATION

Detailed description of computational methods

ALMO DFT. Implementation of energies and FORCES in CP2K with a quick review of its dual-basis feature.

Settings. All AIMD simulations were performed using the dispersion-corrected [26] BLYP exchange-correlation functional [27], large TZV2P Gaussian basis set, 320 Ry cut-off energy for the plane basis set, and GTH pseudopotentials [36, 37]. The size of a periodic cubic simulation box containing 125 water molecules was set to reproduce the experimental $0.997 \text{ g}\cdot\text{cm}^{-3}$ density

of ambient liquid water. The temperature of simulations was set to 298 K and was controlled by a weakly-coupled canonical velocity re-scaling thermostat [38] with the coupling time constant set to 300 fs. A short time step of 0.5 fs ensured accurate integration of the equations of the motion. The total length of simulations for each system was above 7 ps after a equilibrium period of 1.5 ps.

The properties of water including the infrared spectrum, radial distribution, dipole distribution and mean-square deviation were calculated from the MD trajectories using the TRAVIS package [39].

Evaluation of the diffusion constant and viscosity coefficient

The diffusion constant for a periodic system is known to have strong dependence on the size of the simulation box, due to the interaction of a particle with its periodic images [32]. And the diffusion constant obeys:

$$D(\infty) = D(L) + \frac{k_B T \zeta}{6\pi\eta L}, \quad (3)$$

where $D(L)$ is the diffusion constant for a system of size L , η is the translational shear viscosity, and ζ is a constant of 2.837. We calculate the diffusion constant from the mean square deviation of the molecules, for systems of 64, 125, and 256 molecules, and find the viscosity through the dependence of $D(L)$ on $1/L$, which is shown in Fig 5.

Density dependence of localized system

This system will be denoted by low density localized system.

Here we present the calculation of the system at a density of the NPT ensemble at 1atm, which is 0.85g/cm³. The O-O and O-H radial distribution function is shown in Fig 8. The position of the peak doesnot move much for the O-O distritution but the peak is more shallow for the low density system. O-H distance tends to be further in the low density system.

Then angular distribution is shown in Fig 9. Although the interaction for the low density system is weaker, the angular distribution is slightly more ordered. The IR spectrum for the 2 systems are almost identical, as shown in Fig 10.

Basis set dependence of the results

It is know that a straightforward utilization of ALMOs in energy decomposition methods may underestimate charge-transfer effects especially if large basis sets are

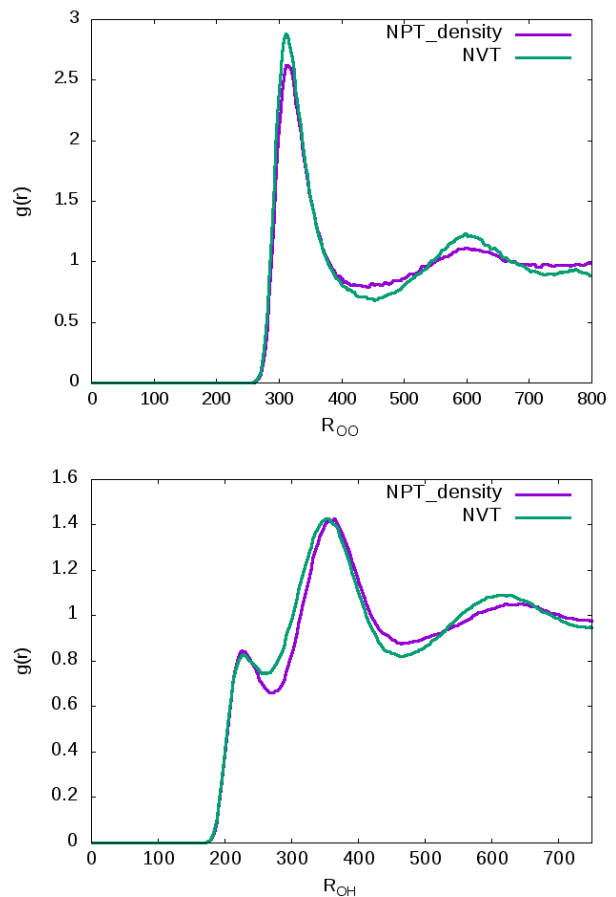


FIG. 8: O-O and O-H radial distribution function for the 2 systems. The cutoff for the O-H distance is set to be 2.6Å.

used [40?]. This deficiency arises from the lack a well-defined separation between the polarization and charge transfer effects in the original ALMO EDA method [17] in the complete basis set limit. It has been demonstrated This problematic aspect of ALMO EDA has been recently be corrected by selecting an appropriated subset of acceptor orbitals[40]. To ensure that our results are not effected by changes in the size of the basis set we re-run AIMD simulation with a larger aug-TZV2P basis set. ZZZ and compare the results with the calculation of TZV2P basis set, which is used otherwise in this work. The results are summarized in Fig 11.

Moreover, TZV2P basis set has been shown to give [quantitatively] accurate description of CT effect in zero-temperature water cluster. It is also important to note that AIMD simulations become unstable if larger basis sets (eg. QZV) are used to model liquid water. This is because of frequent appearance of molecular configuration with linear dependencies in the basis set.

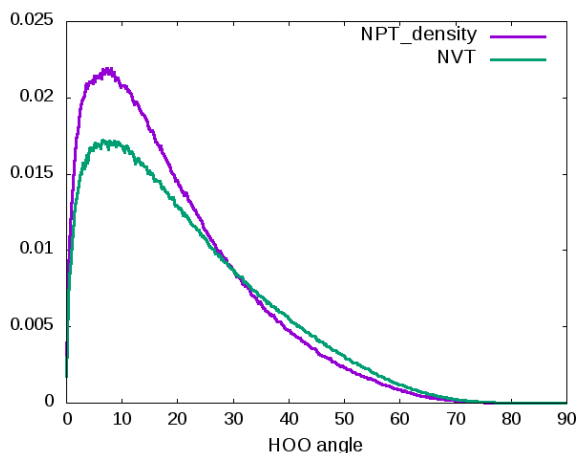


FIG. 9: Angular distribution function for the 2 systems.

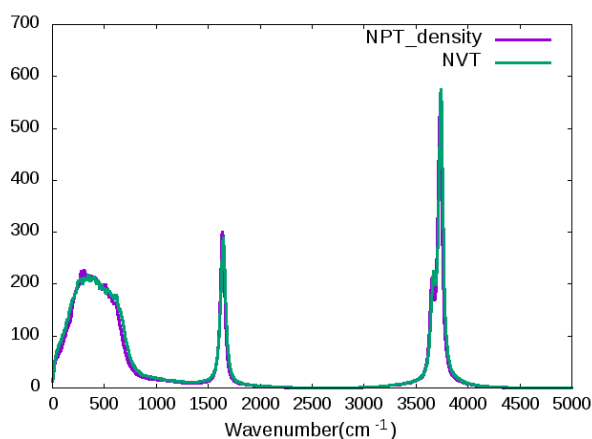


FIG. 10: IR spectrum for the 2 systems.

ACKNOWLEDGMENTS

The research was funded by the Natural Sciences and Engineering Research Council of Canada through the Discovery Grant. The authors are grateful to Compute Canada and McGill HPC Centre for computer time.

[1] D. Eisenberg and W. Kauzmann, *The structure and properties of water* (Oxford University Press on Demand, 2005).
 [2] E. Isaacs, A. Shukla, P. Platzman, D. Hamann, B. Barbiellini, and C. Tulk, *Physical Review Letters* **82**, 600 (1999).
 [3] T. K. Ghanty, V. N. Staroverov, P. R. Koren, and E. R. Davidson, *Journal of the American Chemical Society* **122**, 1210 (2000).
 [4] A. J. Stone, *The Journal of Physical Chemistry A* **121**, 1531 (2017).
 [5] F. Weinhold, *Encyclopedia of computational chemistry*

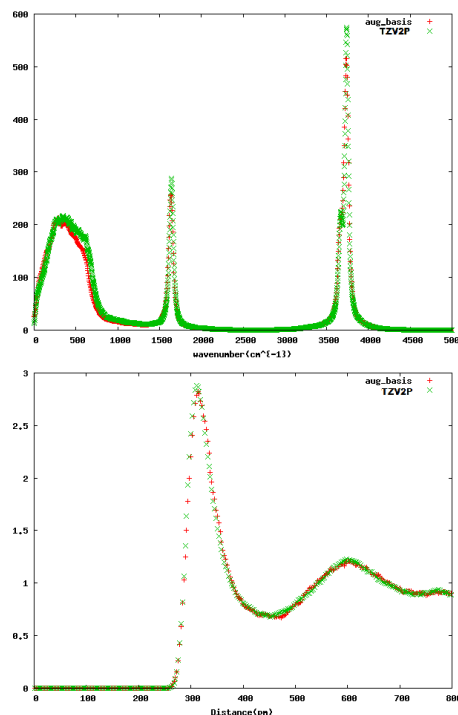


FIG. 11: IR and RDF with aug-TZV2P basis set

(1998).
 [6] E. D. Glendening and A. Streitwieser, *The Journal of chemical physics* **100**, 2900 (1994).
 [7] G. K. Schenter and E. D. Glendening, *The Journal of Physical Chemistry* **100**, 17152 (1996).
 [8] E. D. Glendening, *The Journal of Physical Chemistry A* **109**, 11936 (2005).
 [9] F. Weinhold, *Advances in protein chemistry* **72**, 121 (2005).
 [10] K. Kitaura and K. Morokuma, *International Journal of Quantum Chemistry* **10**, 325 (1976).
 [11] P. S. Bagus, K. Hermann, and C. W. Bauschlicher Jr, *The Journal of chemical physics* **80**, 4378 (1984).
 [12] P. S. Bagus and F. Illas, *The Journal of chemical physics* **96**, 8962 (1992).
 [13] W. J. Stevens and W. H. Fink, *Chemical physics letters* **139**, 15 (1987).
 [14] W. Chen and M. S. Gordon, *The Journal of Physical Chemistry* **100**, 14316 (1996).
 [15] Y. Mo, J. Gao, and S. D. Peyerimhoff, *The Journal of Chemical Physics* **112**, 5530 (2000).
 [16] A. J. Misquitta, B. Jeziorski, and K. Szalewicz, *Physical review letters* **91**, 033201 (2003).
 [17] R. Z. Khaliullin, E. A. Cobar, R. C. Lochan, A. T. Bell, and M. Head-Gordon, *The Journal of Physical Chemistry A* **111**, 8753 (2007).
 [18] J.-P. Piquemal, A. Marquez, O. Parisel, and C. Giessner-Prettre, *Journal of computational chemistry* **26**, 1052 (2005).
 [19] R. Z. Khaliullin, A. T. Bell, and M. Head-Gordon, *Chemistry—A European Journal* **15**, 851 (2009).
 [20] E. A. Cobar, P. R. Horn, R. G. Bergman, and M. Head-Gordon, *Physical Chemistry Chemical Physics* **14**, 15328 (2012).

- [21] T. D. Kühne and R. Z. Khaliullin, arXiv preprint arXiv:1301.4592 (2013).
- [22] C. Zhang, R. Z. Khaliullin, D. Bovi, L. Guidoni, and T. D. Kuhne, The Journal of Physical Chemistry Letters **4**, 3245 (2013).
- [23] H. Elgabarty, R. Z. Khaliullin, and T. D. Kühne, Nature communications **6** (2015).
- [24] R. Z. Khaliullin, J. VandeVondele, and J. Hutter, Journal of chemical theory and computation **9**, 4421 (2013).
- [25] R. Z. Khaliullin, M. Head-Gordon, and A. T. Bell, The Journal of chemical physics **124**, 204105 (2006).
- [26] S. Grimme, J. Antony, S. Ehrlich, and H. Krieg, The Journal of chemical physics **132**, 154104 (2010).
- [27] A. D. Becke, Physical review A **38**, 3098 (1988).
- [28] J. VandeVondele and J. Hutter, The Journal of chemical physics **127**, 114105 (2007).
- [29] T. D. Kuhne and R. Z. Khaliullin, Journal of the American Chemical Society **136**, 3395 (2014).
- [30] E. Arunan, G. R. Desiraju, R. A. Klein, J. Sadlej, S. Scheiner, I. Alkorta, D. C. Clary, R. H. Crabtree, J. J. Dannenberg, P. Hobza, et al., Pure and applied chemistry **83**, 1637 (2011).
- [31] M. W. Mahoney and W. L. Jorgensen, The Journal of Chemical Physics **112**, 8910 (2000).
- [32] B. Dünweg and K. Kremer, The Journal of chemical physics **99**, 6983 (1993).
- [33] M. Neumann, Molecular Physics **50**, 841 (1983).
- [34] D. J. Adams, Nature **293**, 447 (1981).
- [35] Y. Maréchal, *The hydrogen bond and the water molecule: The physics and chemistry of water, aqueous and bio-media* (Elsevier, 2006).
- [36] S. Goedecker, M. Teter, and J. Hutter, Physical Review B **54**, 1703 (1996).
- [37] M. Krack, Theoretical Chemistry Accounts: Theory, Computation, and Modeling (Theoretica Chimica Acta) **114**, 145 (2005).
- [38] G. Bussi, D. Donadio, and M. Parrinello, The Journal of chemical physics **126**, 014101 (2007).
- [39] M. Brehm and B. Kirchner, Journal of cheminformatics **4**, F1 (2012).
- [40] P. R. Horn and M. Head-Gordon, The Journal of chemical physics **143**, 114111 (2015).